

Glucose supply and glycolysis inhibition shape the clinical fate of *Staphylococcus epidermidis*-infected preterm newborns

Tik Muk, Anders Brunse, Nicole L. Henriksen, Karoline Aasmul-Olsen, and Duc Ninh Nguyen

Section for Comparative Pediatrics and Nutrition, Department of Veterinary and Animal Sciences, University of Copenhagen, Copenhagen, Denmark.

Preterm infants are susceptible to bloodstream infection by coagulase-negative staphylococci (CONS) that can lead to sepsis. Glucose-rich parenteral nutrition is commonly used to support the infants' growth and energy expenditure but may exceed endogenous regulation during infection, causing dysregulated immune response and clinical deterioration. Using a preterm piglet model of neonatal CONS sepsis induced by *Staphylococcus epidermidis* (*S. epidermidis*) infection, we demonstrate the delicate interplay between immunity and glucose metabolism to regulate the host infection response. Circulating glucose levels, glycolysis, and inflammatory response to infection are closely connected across the states of tolerance, resistance, and immunoparalysis. Furthermore, high parenteral glucose provision during infection induces hyperglycemia, elevated glycolysis, and inflammation, leading to metabolic acidosis and sepsis, whereas glucose-restricted individuals are clinically unaffected with increased gluconeogenesis to maintain moderate hypoglycemia. Finally, standard glucose supply maintaining normoglycemia or pharmacological glycolysis inhibition enhances bacterial clearance and dampens inflammation but fails to prevent sepsis. Our results uncover how blood glucose and glycolysis control circulating immune responses, in turn determining the clinical fate of preterm infants infected with CONS. Our findings suggest further refinements of the current practice of parenteral glucose supply for preterm infants during infection.

Introduction

Among millions of infants born preterm (i.e., <37 weeks of gestation) every year, 25%–50% of those with very low birth weight experience serious neonatal infection, leading to sepsis (1). Up to 80% episodes of late-onset sepsis (i.e., >3 days after birth) are caused by coagulase-negative staphylococci (CONS), especially *Staphylococcus epidermidis* (*S. epidermidis*) (2–4). Although CONS-associated sepsis is not as life-threatening as Gram-negative bacterial sepsis, it is of serious concern as a predisposing factor to multiple morbidities occurring later in life (5, 6). Currently, the only therapeutic option for neonatal infection is antibiotics, which are empirically used for almost all preterm infants (7, 8) despite the risk of disturbing immune development and causing antimicrobial resistance (9).

The interplay between immune cell energy metabolism and function has emerged as a key mechanism in many adult diseases, but its role in neonatal infection is largely unknown. Initial theories (10, 11) and in vitro reports (12, 13) suggest that the low energy reservoir in newborns programs their immune system to disease tolerance — a strategy avoiding fast ATP production for inflammatory responses in immune cells via inhibition of the Warburg effect switching from oxidative phosphorylation (OXPHOS) to glycolysis. This may explain how newborns tolerate 10–100 times higher systemic bacterial loads (10) and have diminished blood cytokine responses to in vitro infection challenge (14, 15), relative to adults. However, it is unclear how this disease tolerance in preterm infants is connected to their high susceptibility to neonatal sepsis, a pathological state associated with an early hyperinflammatory phase followed by immunoparalysis or death (16).

During the first few weeks of life, a majority of preterm infants receive parenteral nutrition (PN) to maintain adequate nutrition, and international guidelines recommend a parenteral supplement containing a high concentration of glucose (~14–17 g/kg/d) to avoid hypoglycemia (i.e., blood glucose level <2.6 mM) and related brain injury (17–20). However, prolonged high parenteral glucose intake may lead to

Authorship note: TM and AB are co-first authors.

Conflict of interest: The authors have declared that no conflict of interest exists.

Copyright: © 2022, Muk et al. This is an open access article published under the terms of the Creative Commons Attribution 4.0 International License.

Submitted: December 3, 2021

Accepted: April 29, 2022

Published: June 8, 2022

Reference information: *JCI Insight*.

2022;7(11):e157234.

<https://doi.org/10.1172/jci.insight.157234>.

insight.157234.

hyperglycemia (i.e., blood glucose level >6.9 mM) (21), which is detected in up to 80% of preterm infants (22). Notably, there are no specific guidelines for using parenteral glucose during neonatal infection, although PN-related hyperglycemia is associated with longer hospitalization of infected infants (18). We postulate that high parenteral glucose provision to infected newborns may accelerate blood immune cell glycolysis, leading to excessive inflammation and sepsis. Detailed understanding of this mechanism may shed light on novel infection therapies (e.g., reduced parenteral glucose supply or glycolysis inhibition).

Numerous animal models of infection and sepsis have been established e.g., cecal ligation and puncture (23) and oral (24, 25) or systemic bacterial challenge (26), but no rodent models can address the contributing effects of PN. The preterm pig is a unique model because it allows PN administration via umbilical catheter (27) and has multiple organ immaturities and infection susceptibility (26, 28–30), as found in preterm infants. Furthermore, systemic *S. epidermidis* administration to newborn preterm pigs can induce clinical and cellular responses (e.g., fever, inflammation, blood platelet and leukocyte depletion) that may progress to septic shock (acidemia and hypotension) 12–24 hours after infection, similar to sepsis caused by CONS and other bacteria in preterm infants (26). Here, we further used this CONS sepsis model and showed that the infection response in preterm newborns was tightly related to circulating glycolysis and glucose levels. We found that high parenteral glucose supply predisposed to hyperglycemia, excessive inflammation, reduced bacterial clearance, and extreme sensitivity to sepsis following neonatal infection, whereas restricted glucose provision caused hypoglycemia but protected against sepsis. We also showed that a standard glucose supply maintaining normoglycemia, with or without using a glycolysis inhibitor, dichloroacetate (DCA), enhanced bacterial clearance and alleviated systemic inflammation and metabolic acidosis but did not prevent sepsis. Parenteral glucose restriction may be an effective therapy for preterm infants infected with CONS.

Results

S. epidermidis thresholds determine the host immunometabolic responses in vitro and in vivo. Preterm infants can presumably withstand higher circulating bacterial levels than can adults and term infants prior to mounting resistant responses and later becoming immunoparalyzed (10). Here, we first tested the threshold switching among those phases by measuring in vitro immunometabolic responses of cord blood from preterm pigs to increasing doses of *S. epidermidis* (Figure 1). When increasing bacterial doses, inflammatory (TNF- α) and antiinflammatory (IL-10) cytokine responses at both the gene and protein levels switched from an immune-tolerant state at low doses (5×10^1 to 5×10^4 CFU/mL) to resistance at the dose of 5×10^5 CFU/mL (Figure 1, A–C, and Supplemental Figure 1, A–C; supplemental material available online with this article; <https://doi.org/10.1172/jci.insight.157234DS1>). Of note, the ratio of *TNFA* to *IL10* (Th1 and Th2 cytokines, respectively) also peaked at 5×10^5 CFU/mL but decreased again at higher doses, indicating another switch to immunoparalysis. The same trends applied to other parameters, including elevated mRNA levels of targets related to inflammation (*IL6*, *TLR2*), Th1 responses (*IFNG* and *IFNG/IL4*), and the glycolysis–mTOR pathway (*HIF1A*); and decreased levels of genes related to OXPHOS (*COX1*) and Foxp3⁺CD4⁺ lymphocytes (a Treg marker) at the bacterial dose of 5×10^5 CFU/mL but not lower or higher doses (Figure 1, D–I, and Supplemental Figure 1, D and E). In parallel, cellular glucose uptake, measured by the differences in supernatant glucose levels with versus without bacterial challenge, was gradually elevated with increasing bacterial doses, then reached a plateau level at the bacterial dose of 5×10^5 CFU/mL (Supplemental Figure 1F). These data revealed clear dose-dependent switches of immunometabolic response to *S. epidermidis* from tolerance to resistance and, later, immunoparalysis.

We then tested clinical and metabolic responses to increasing *S. epidermidis* doses in vivo, using newborn preterm pigs (at 90% gestation) nourished by PN with a standard glucose (STG) level. The animals were clinically and metabolically unaffected by the 2 lowest doses (10^6 and 10^8 CFU/kg; disease tolerance). At a dose of 10^9 CFU/kg, survival was 75% with dysregulated glucose and lactate at 24-hour follow-up (i.e., disease resistance), whereas the highest dose of 5×10^9 CFU/kg decreased the 24-hour survival rate to less than 20% and induced glucose and lactate dysregulation already at 12 hours (Figure 2, A–C). Plasma IL-6 and IL-10 at 24 hours after infection showed increased levels with increasing doses of inoculated bacteria (Figure 2, D and E). Thus, clinical responses were clearly intertwined with perturbed glucose homeostasis and followed a severity spectrum dictated by bacterial dose and cytokine responses. Furthermore, to confirm the metabolic shifts following infection, we performed a follow-up experiment and collected liver of infected (10^9 CFU/kg) and control animals for transcriptomic analysis. The liver of infected animals clearly showed activation of both inflammatory pathways (i.e., TNF and

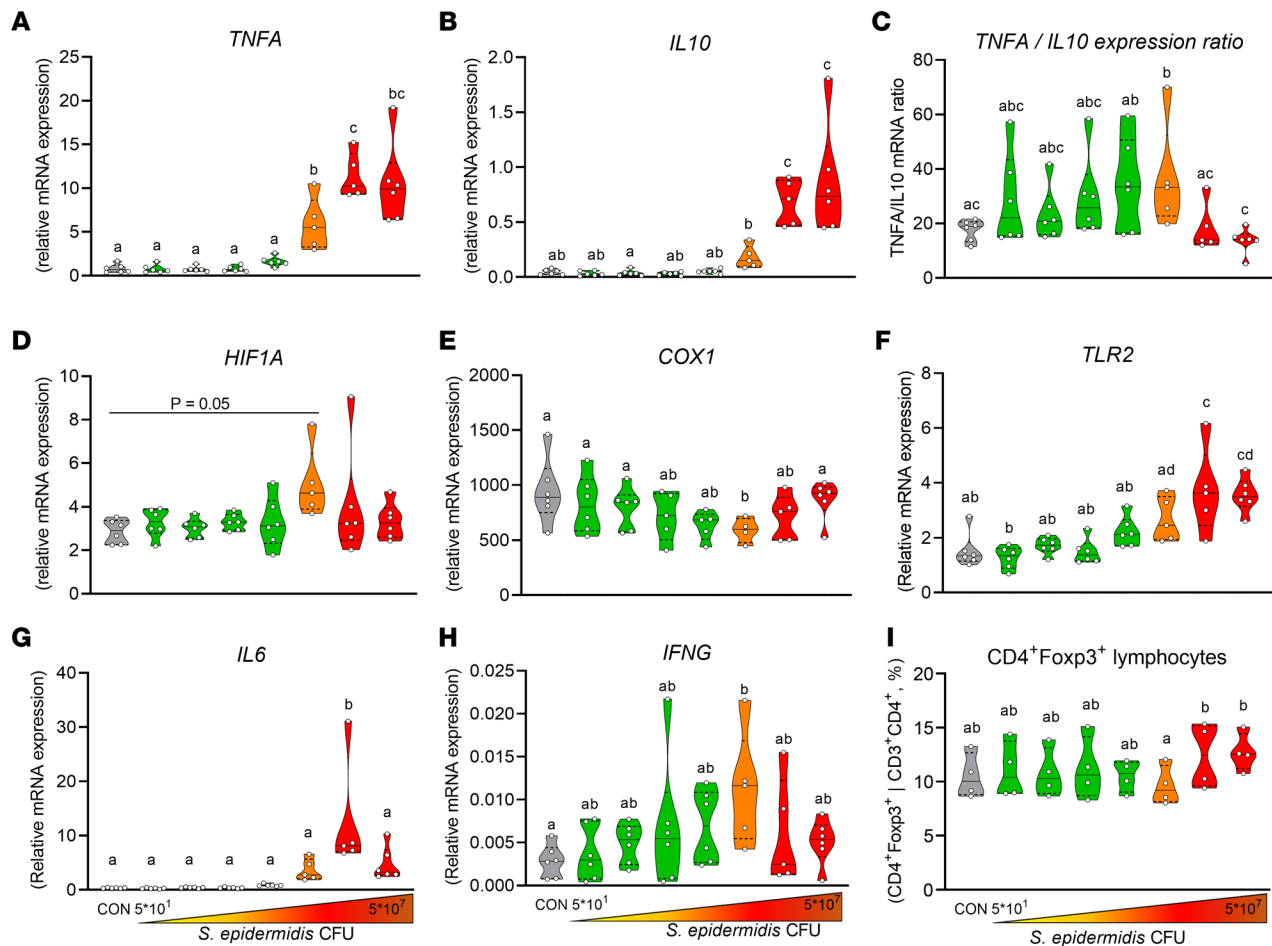


Figure 1. In vitro immunometabolic response to *S. epidermidis*. (A–H) mRNA levels of *TNFA*, *IL10*, *TNFA* to *IL10* ratio, *HIF1A*, *COX1*, *TLR2*, *IL6*, and *IFNG* of cord blood from preterm piglets in responses to an increasing bacterial dose (5×10^1 to 5×10^7 CFU/mL, stimulated for 2 hours at 37°C and 5% CO_2 ; $n = 5$ –6). (I) Frequency of CD4^+ lymphocyte population in *S. epidermidis*-stimulated cord blood (2 hours at 37°C and 5% CO_2 ; $n = 4$). All data are presented as violin dot plots with median (solid line) and IQR (dotted lines) and were analyzed using a linear mixed-effect model followed by Tukey post hoc comparisons. Values not sharing the same letters are significantly different ($P < 0.05$).

IL-17 signaling, Th1 and Th1 differentiation) and sugar metabolic pathways (i.e., glycolysis, galactose, fructose and mannose metabolism) (Figure 2F; Supplemental Figure 1, G and H; and Supplemental Table 1, A and B). Both in vitro and in vivo data showed that preterm immune cells had a propensity to undergo a metabolic shift toward aerobic glycolysis when activated, whereby glucose availability may determine the potency of cellular and cytokine responses with potential clinical implications.

*Parenteral glucose determines sepsis susceptibility during *S. epidermidis* infection.* We next investigated clinical, metabolic, and immune responses to neonatal systemic infection on the background of experimentally extreme differences in glucose provision to mimic hyperglycemic and hypoglycemic conditions in infected preterm infants. Newborn preterm piglets were nourished exclusively with PN containing either a high glucose (HG; 21% glucose) or a very low glucose (LG; 1.4% glucose) level, and we systemically challenged the piglets with 10^9 CFU/kg *S. epidermidis*, the dose leading to clinical symptoms but moderate acute mortality from the dose-finding study (experimental design in Figure 3A). Based on the criteria for sepsis and the humane euthanasia endpoint for this study (i.e., arterial blood pH < 7.1 and clinical symptoms of extreme lethargy, discoloration, and tachypnea), animals receiving HG PN (hereafter, HG animals) at the end of the study (12 hours) had substantially higher sepsis incidence and mortality relative to those of animals receiving LG (hereafter, LG animals) (HG vs. LG: $n = 10$ of 11 vs. $n = 2$ of 10; $P < 0.01$) (Figure 3B). Importantly, these findings were accompanied by impaired blood bacterial clearance dynamics from 3 to 12 hours in the HG animals (P for glucose levels [P_{glu}] < 0.01) (Figure 3C), whereas LG PN prevented respiratory and metabolic acidosis by preserving blood acid-buffering capacity (for all, $P_{\text{glu}} < 0.01$) (Figure 3, D–F).

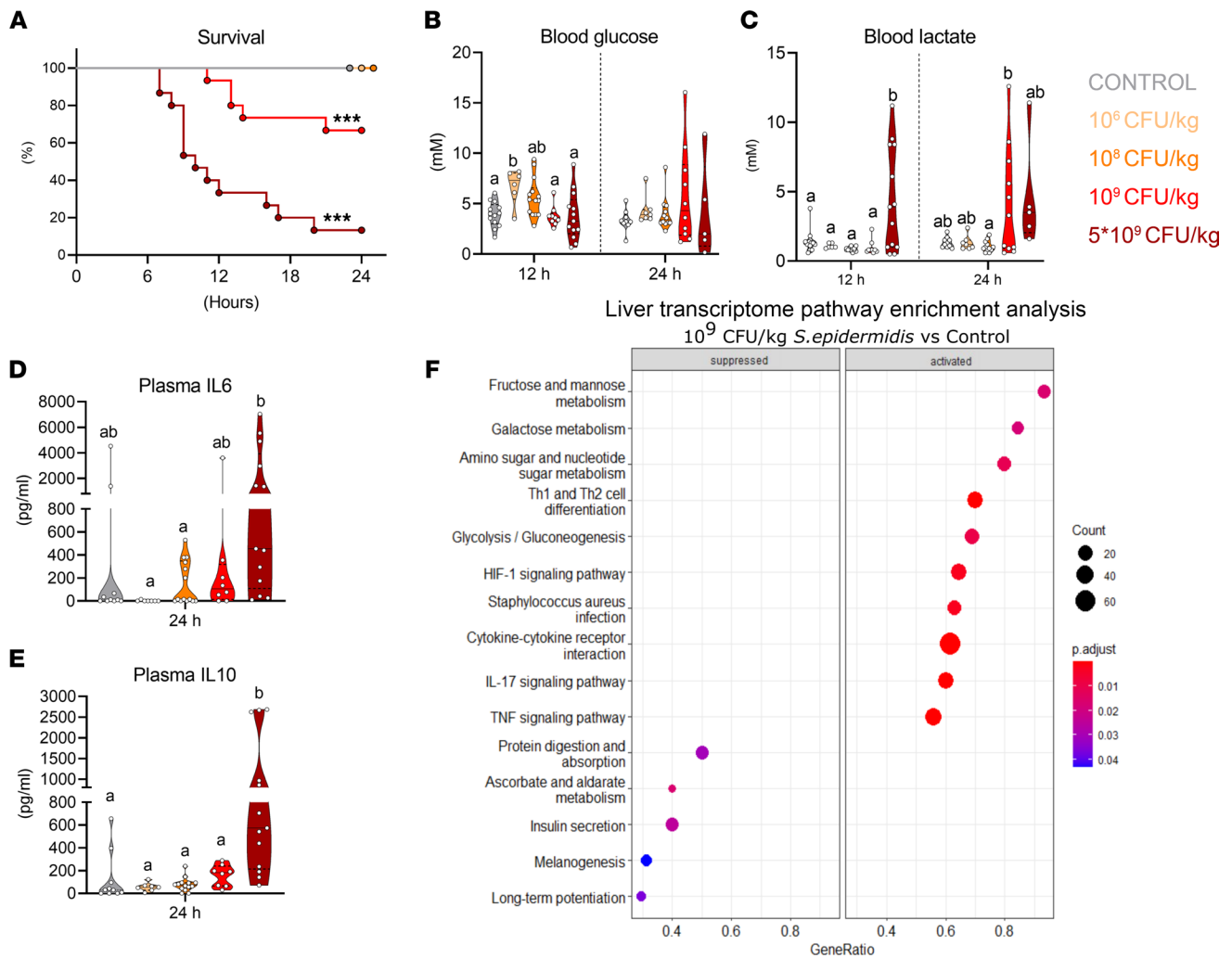


Figure 2. In vivo immunometabolic response to *S. epidermidis*. (A) Survival rate, (B) blood glucose, (C) lactate, (D) plasma IL-6, and (E) plasma IL-10 levels of preterm newborn piglets 24 hours after infection with *S. epidermidis* (10^6 to 5×10^9 CFU/kg) via the intra-arterial catheter. (F) Gene set enrichment analysis (GSEA) of liver transcriptome from control and *S. epidermidis*-infected preterm pigs (10^9 CFU/kg, 12 hours after infection) revealing the top enriched pathways activated and suppressed by infection. Data are presented in a cumulative hazard curve (A) or violin dot plots with median (solid line) and IQR (dotted lines, B–E), and analyzed by Mantel-Cox test or linear model followed by Tukey post hoc comparisons. Values at a time point not sharing the same letters are significantly different ($P < 0.05$). $***P < 0.001$, compared with the uninfected control. Transcriptomics was performed by DESeq2 with FDR adjusted by BH correction using $\alpha = 0.1$ as the threshold. GSEAs were based on DEGs between infected and control groups, and pathways with adjusted (adjust.) $P < 0.05$ are considered significantly regulated pathways. Gene ratio (from 0 to 1) shows the fraction of the number of enriched genes relative to the total number of genes in the gene set. The size of the circle reflects the number of DEGs enriched in each pathway.

Moreover, HG piglets had a quicker meconium passage than did LG animals, a common physiological stress response in the perinatal period (Figure 3I). Furthermore, plasma albumin levels by the end of the study were 2 times lower in the HG piglets relative to LG piglets ($P < 0.01$), indicating stress-induced changes in liver protein synthesis, vascular permeability, or renal dysfunction. Taken together, glucose restriction during neonatal *S. epidermidis* infection provided acute clinical benefits.

Unsurprisingly, HG piglets were hyperglycemic (blood glucose level of 10–20 mM) with an increasing trend over time, whereas the LG nourishment paradigm led to hypoglycemia, with blood glucose levels of approximately 2 mM and a decreasing time trend (Figure 3G). A similar pattern was observed for blood lactate: 40% of animals in the HG group had levels greater than 10 mM ($P < 0.01$ at 12 hours vs. LG group) (Figure 3H), indicating accelerated circulating glycolysis and lactic acidosis, whereas lactate levels in the LG group decreased over time, likely because it was used for gluconeogenesis. Despite a large difference in plasma glucose levels, ATP and pyruvate levels only showed minor or no differences between the HG and LG groups (Figure 3, J and K). However, blood urea levels at 12 hours were markedly increased in LG relative to HG

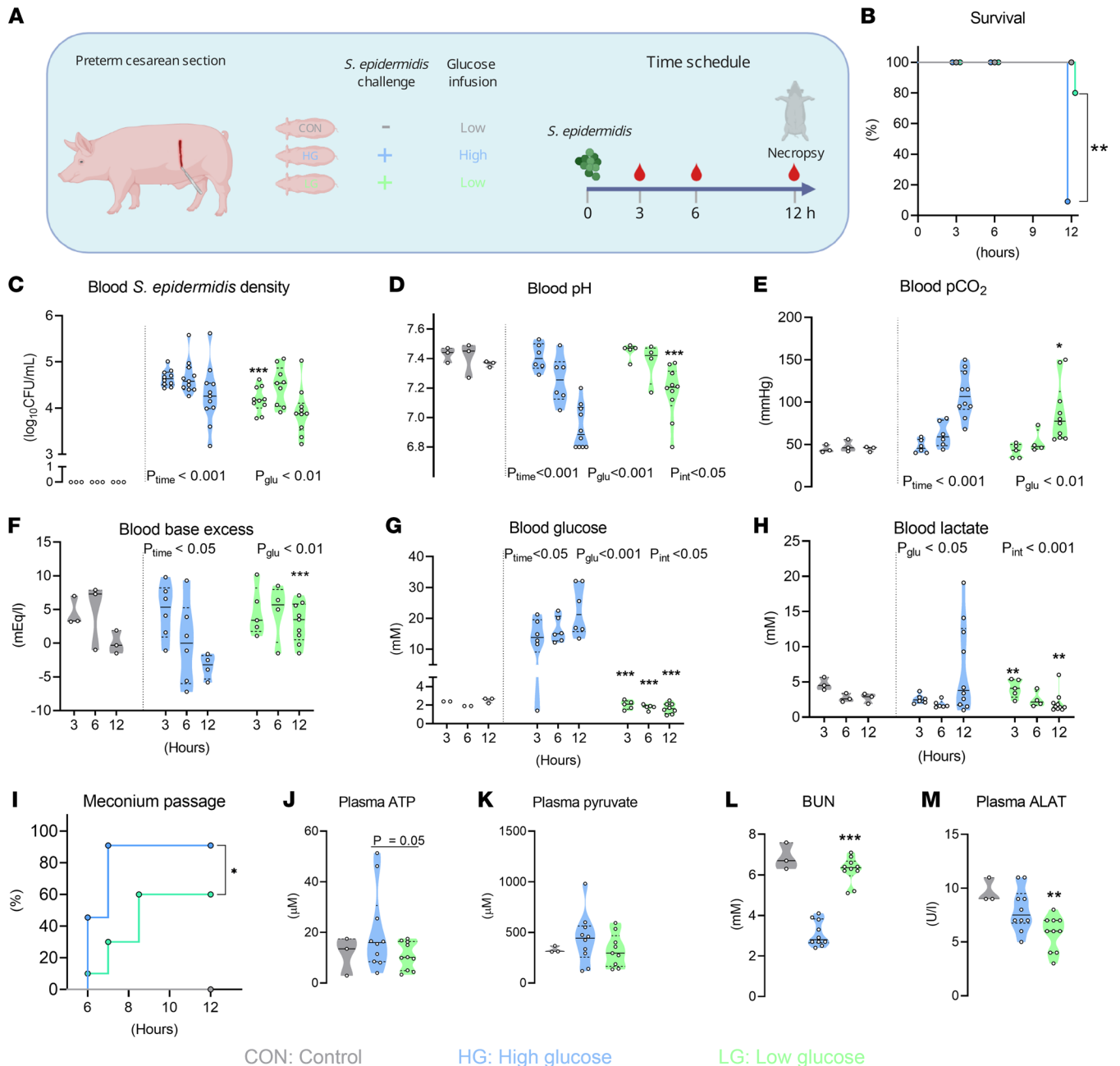


Figure 3. Parenteral glucose restriction protects *S. epidermidis*-infected preterm piglets from sepsis. (A) Preterm newborn piglets were nourished exclusively with PN containing HG (21%; 30 g/kg/d) or LG (1.4%; 2 g/kg/d) concentrations ($n = 10$ –11 per group), intra-arterially infected with 10^9 CFU/kg *S. epidermidis*, and cared for 12 hours after infection or until clinical signs of sepsis. Uninfected animals ($n = 3$) receiving LG PN served as a reference and were not included in the statistics. (B) Survival curve, based on sepsis diagnosis and humane euthanasia endpoint (i.e., blood pH < 7.1 and presence of septic shock symptoms). (C) *S. epidermidis* density from blood collected by jugular venous (3–6 hours) or heart (12 hours) puncture, by counting CFUs after plating onto tryptic soy agar containing 5% sheep's blood and incubated for 24 hours at 37°C. (D–H) Blood-gas parameters derived from arterial blood samples collected via the umbilical arterial catheter at 3, 6, and 12 hours. (I) Time of first passed meconium after infection. (J–M) Blood biochemical parameters measured in heparinized plasma from arterial blood collected at 12 hours. Data are presented as cumulative hazard curves (B and I) or violin dot plots including median (solid line) and IQR (dotted lines) (C–H and J–M). Data were analyzed using a Mantel-Cox test (B and I) or a linear mixed-effects model (C–H and J–M), including an interaction between group and time after infection (C–H). All analyzed data represent 2 independent litters. P for time (P_{time}), P_{glu} , and P for interaction (P_{int}) denote probability values for effects over time across the HG and LG groups, group effect (HG vs. LG) over time, and interaction effect between time and group in the linear mixed effects interaction model, respectively. * $P < 0.05$, ** $P < 0.01$, *** $P < 0.001$, compared with HG group at the same time point. ALAT, alanine aminotransferase; BUN, blood urea nitrogen; CON, control; pCO_2 , partial pressure of CO_2 . Panel A was created using Biorender.com.

animals (Figure 3L), suggesting conversion of exogenous glucogenic amino acids to fuel endogenous glucose production. In parallel, the plasma activity of alanine aminotransferase, the enzyme responsible for deaminating alanine to pyruvate as an initial step in gluconeogenesis, was decreased in the LG group (Figure 3M). In summary, high parenteral glucose provision during infection facilitated extensive circulating glycolysis, whereas acute metabolic adaptation to exogenous glucose restriction appeared to maintain adequate cellular energy.

During the 12-hour course of infection, glucose infusion levels massively interfered with the fate of blood cell subsets. An overall decreasing trend in cell numbers was observed over time for leukocytes, erythrocytes, and thrombocytes (Figure 4, A–C), with HG PN leading to a greater loss of total leukocytes and more severe thrombocytopenia ($P_{\text{glu}} < 0.01$). Importantly, HG PN induced a robust depletion of lymphocytes, neutrophils, and monocytes at 3–6 hours with partial replenishment at 12 hours, which was not observed in the LG group (Figure 4, D–F). Interestingly, this was associated with distinct temporal changes in plasma cytokine response to infection. TNF- α , IL-10, and IL-6 levels were elevated over time during infection, but HG animals had more pronounced TNF- α and IL-6 responses and lower IL-10 levels relative to LG group ($P_{\text{glu}} < 0.01$) (Figure 4, G–I). Collectively, the HG nourishment paradigm induced a more rapid immune response with greater cell loss and evidence of emergency hematopoiesis, prioritizing release of leukocytes but not erythrocytes and thrombocytes from the bone marrow. This may have compromised the regulatory response shown by reduced IL-10 secretion.

Although glucose restriction has acute clinical benefits with reduced mortality and clinical signs of sepsis, glycolysis, and systemic inflammation, this practice led to hypoglycemia and may have negative effects on the preterm brain, which relies on steady glucose supplies for proper development. Therefore, an alternative strategy to manipulate the immunometabolic response to infection in a normo- or hyperglycemic state was investigated.

Glycolysis inhibition decreases inflammatory response to S. epidermidis in vitro. Having shown that circulating glycolysis is closely connected to inflammation and clinical fate during neonatal *S. epidermidis* infection, we aimed to identify a clinically relevant treatment to prevent sepsis and exaggerated aerobic glycolysis beyond glucose restriction. First, we tested the well-known glycolysis inhibitors at their commonly used doses found in the literature for capacity to reduce inflammation in preterm pig cord blood challenged with *S. epidermidis*. Rapamycin (which targets the mTOR pathway), DCA (which targets pyruvate dehydrogenase kinase), and FX11 (which targets lactate dehydrogenase) all reduced bacteria-induced TNF- α response, but DCA seemed to have higher inhibitory potency across the 2 tested bacterial doses (Figure 5A). We proceeded with a dose-finding test for DCA (0.1–10 mM), a water-soluble molecule with a short half-life and widely used for patients with cancer and diabetes (31) to suppress inflammation, with limited adverse effects (32). Relative to lower doses, DCA at 10 mM was more effective to decrease *S. epidermidis*-induced TNF- α secretion (Figure 5B) and expression of hexokinase 2 (an enzyme facilitating the first reaction of glycolysis pathway) and CXCL8 (a proinflammatory chemokine) (Supplemental Figure 2, A–C). Importantly, preterm cord blood treated with DCA had increased neutrophil phagocytic capacity under both normo- and hyperglycemic conditions (Figure 5C), but DCA did not exert direct bacterial growth inhibitory effect in bacterial culture medium (Figure 5D), nor did it decrease overall bacterial density in *S. epidermidis*-stimulated cord blood (Figure 5E).

We further performed RNA-Seq analysis of *S. epidermidis*-stimulated cord blood with and without DCA addition (Figure 5, F–J; Supplemental Table 2, A–H; and Supplemental Figure 3) and observed clear effects of bacterial stimulation ($n = 90$ differentially expressed genes [DEGs]) and DCA treatment in stimulated samples ($n = 239$ DEGs). The bacterial challenge upregulated genes and pathways related to innate and adaptive immune activation and downregulated genes involved in OXPHOS (Figure 5, G and H). Conversely, comparing the 2 bacteria-stimulated groups, DCA upregulated antiinflammatory and OXPHOS pathways, and downregulated inflammatory pathways (Figure 5, G–I). DCA also increased expression of genes related to endocytosis and phagocytosis (Figure 5J). Collectively, DCA appeared capable of inhibiting infection-induced immune cell glycolysis and inflammation and, therefore, was selected as our drug candidate for preventing neonatal sepsis under normo- and hyperglycemic conditions.

STG supply and DCA reduce inflammation and improve bacterial clearance but do not prevent sepsis. Having identified glycolysis inhibition by DCA as a potential alternative to glucose restriction, we again used the preterm pig *S. epidermidis* infection model to test the ability of both parenteral glucose supply maintaining normoglycemia and DCA to reduce sepsis incidence and severity, relative to HG supply, in a 2×2 factorial experimental design. The animals were provided PN with STG level (10% glucose) or high parenteral

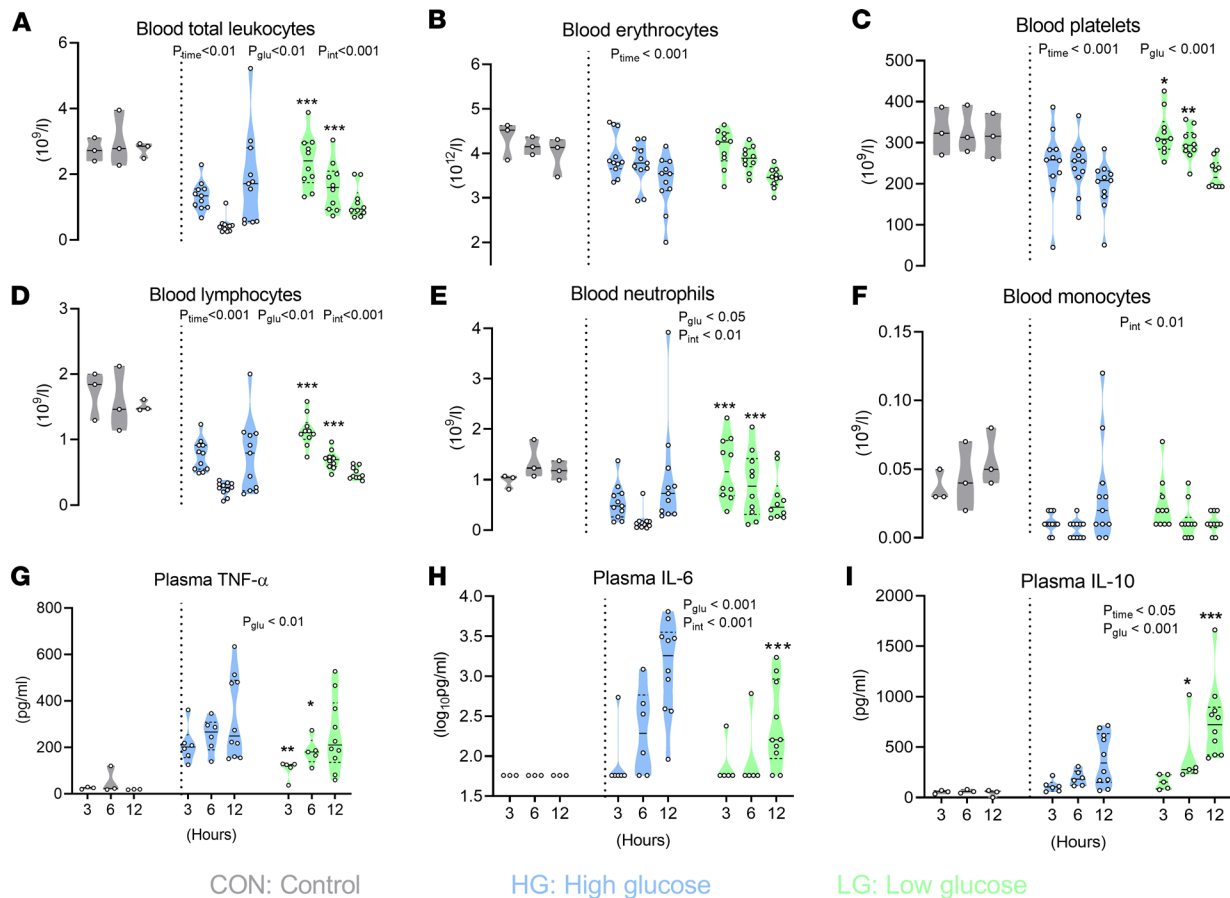


Figure 4. Parenteral glucose restriction protects *S. epidermidis*-infected preterm piglets from excessive inflammation and immune cell loss.

(A–F) Numbers of hematopoietic cells and major leukocyte subsets in blood samples collected 3–12 hours after *S. epidermidis* infusion. (G–I). Cytokine levels measured in heparinized plasma from the same blood samples. Data are presented as violin dot plots with median and IQR and were analyzed using a linear mixed-effects model including interaction between group and time after infection. All analyzed data represent 2 independent experiments using separate litters. P for time (P_{time}), P_{glu} , and P for interaction (P_{int}) denote probability values for time effects across HG and LG groups, group effect (HG vs. LG) over time and interaction effect between time and group in the linear mixed-effects model, respectively. * $P < 0.05$, ** $P < 0.01$, *** $P < 0.001$, compared with HG group at the same time point.

glucose levels (21% glucose), as well as DCA treatment (50 mg/kg) or saline control shortly after *S. epidermidis* infusion (experimental design in Figure 6A). The selected DCA dose was aimed to match the effective dose in vitro and the recommended dose in adult patients with lactic acidosis (33).

Using similar criteria for sepsis and the humane euthanasia endpoint (i.e., blood pH < 7.1 , plus clinical signs), the sepsis incidence and survival rates across the 4 infected groups after 12 hours were similar (22%–44%; $P > 0.05$). The meconium passage time was generally more rapid in this experiment and not affected by DCA treatment but was still delayed in the STG group ($P < 0.05$) (Figure 6B, indicating less stress response) compared with the piglets receiving HG PN with DCA (hereafter, HG-DCA) group. Bacterial clearance 3–12 hours after infection was enhanced by lowering the glucose supply across the infected groups ($P_{glu} < 0.01$) with an indication of best clearance in piglets receiving STG PN with DCA (hereafter, STG-DCA) group (Figure 6C). However, blood pH (the main sepsis indicator) and partial pressure of CO_2 were similar across the 4 infected groups despite trends of better blood acid–base balance in STG and STG-DCA animals (Figure 6D and Supplemental Figure 4, A and B). Unsurprisingly, most HG and HG-DCA animals were hyperglycemic, and most STG and STG-DCA animals were normoglycemic.

We detected an interesting trend of decreased blood glucose levels over time in HG but not HG-DCA pigs (higher at 6 hours in the HG-DCA group vs. the HG group) (Figure 6E). This suggests that blood glucose was used for glycolysis during infection in HG pigs, whereas glycolysis inhibition resulted in reduced cellular glucose uptake and consistent hyperglycemia in HG-DCA pigs. Blood lactate level was reduced effectively only by DCA (P for DCA [P_{DCA}] < 0.05) but not by lowering glucose supply (Figure 6F).

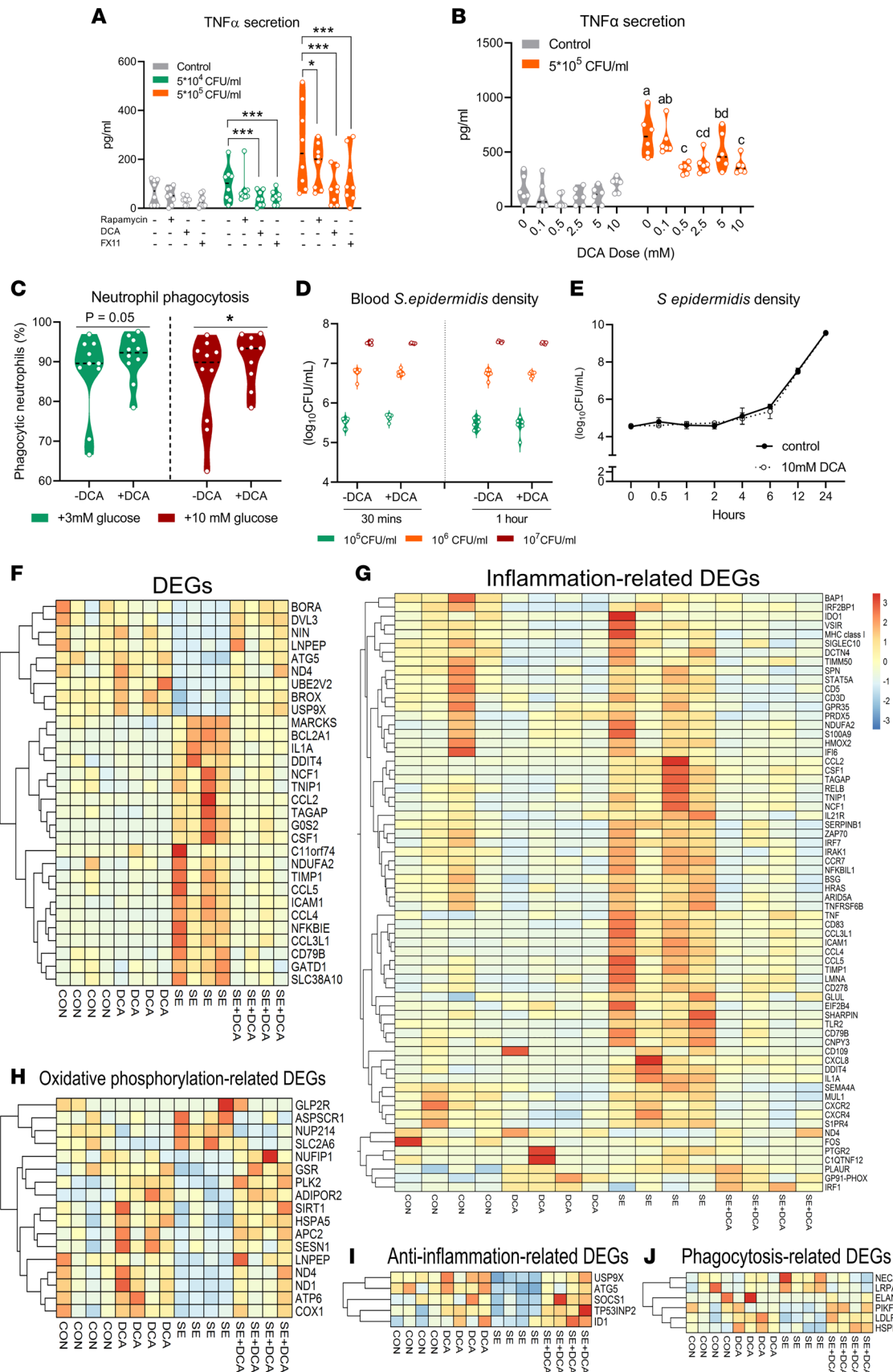


Figure 5. Glycolysis inhibition decreases inflammation in *S. epidermidis*-challenged preterm cord blood. (A and B) TNF- α levels in cord blood of preterm piglets ($n = 6$) following stimulation with *S. epidermidis*, with and without presence of a glycolysis inhibitor: rapamycin (500 nM), DCA (10 mM), and FX11 (100 μ M) at 37°C and 5% CO₂ incubation ($n = 6$) (A); and DCA (0.1–10 mM) (B). (C) Cord blood neutrophil phagocytosis ($n = 10$, from 2 independent litters)

measured by fraction of neutrophils having phagocytic capacity in cord blood with and without 10 mM DCA added at normo- or hyperglycemic conditions. In vitro phagocytosis assay was performed by incubating samples with pHrodo-conjugated *E. coli* for 30 minutes at 37°C and 5% CO₂ and analyzed by flow cytometry. (D) Bacterial density in preterm cord blood following stimulation with *S. epidermidis* (theoretical dose from 10⁵ to 10⁷ CFU/mL) for 30 minutes or 1 hour with and without preincubation with 10 mM DCA (*n* = 6). (E) Effects of DCA (10 mM) on *S. epidermidis* growth (*n* = 3). (F–J) Heatmaps from transcriptomic analyses of cord blood samples with or without *S. epidermidis* (5 × 10⁵ CFU/mL) and DCA incubation. (F) The top 30 DEGs from the comparison between control (CON) and *S. epidermidis*-challenged samples. (G–J) Selective DEGs related to inflammation (G), OXPHOS (H), antiinflammatory effect (I), and phagocytosis and endocytosis (J) and obtained from the comparison between *S. epidermidis*-stimulated samples without versus with DCA addition. For each DEG (row), z-scores of the expression levels are depicted in colors from blue (low) to red (high). (A–E) Data are presented as violin dot plots with median and IQR and were analyzed using a linear mixed-effect model with inhibitor treatment as a fixed factor and pig ID as the random factor. **P* < 0.05, ****P* < 0.001. (B) Values not sharing the same letters are significantly different (*P* < 0.05). SE, *S. epidermidis*.

In parallel, plasma pyruvate and ATP levels, reflecting the degree of energy production enhanced by glycolysis during infection, were lowest in the STG-DCA group (Figure 6, G and H). All these data indicate that DCA effectively reduced glycolysis during infection, but none of the 2 interventions (i.e., DCA or STG supply) reduced clinical sepsis signs, relative to HG supply. This is in contrast with the effective sepsis protection of glucose restriction in the previous experiment.

Reduced PN glucose and DCA treatment also exerted differential effects on blood cell subsets and cytokines. Similar to previous experiments, infection led to reductions of all immune cell subsets, erythrocytes, reticulocytes, and thrombocytes (Figure 7, A–E; and Supplemental Figure 4, C and D). Lowering PN glucose from high to standard levels preserved fractions of lymphocytes, thrombocytes, and reticulocytes (*P*_{glu} < 0.05) but not neutrophils. Among the 4 infected groups, HG-DCA animals had the most severe drops of total numbers of leukocytes, erythrocytes, and thrombocytes, and the highest plasma levels of IL-6, but not IL-10 and TNF-α (Figure 7F and Supplemental Figure 4, E and F). These possibly suggest the negative impact of more severe hyperglycemic conditions caused by DCA in the high parenteral glucose background. Conversely, DCA did not have further beneficial impacts on hematological and cytokine levels in the background of standard glucose supply.

To better understand the effects of lowering glucose supply and DCA at the molecular level, a subset of blood samples collected 12 hours after infection was subjected to RNA-Seq analysis (Figure 8 and Supplemental Table 1, C–K). *S. epidermidis* infection induced dramatic blood transcriptomic changes (21.2% of annotated genes). This included upregulation of 2011 genes and pathways related to innate immunity (i.e., TLR, NOD signaling) and early phase of Th1 polarization (i.e., chemokine and TNF signaling) and downregulation of 1967 genes and pathways related to adaptive immunity (i.e., T and B cell receptor signaling) and metabolism (Figure 8, A and B; and Supplemental Table 1, I–K). Among the 4 infected groups (Supplemental Table 1, C–H), HG pigs possessed a distinct profile of inflammation-related genes, with half of the DEGs being highly upregulated and the other half being downregulated relative to the remaining 3 groups (Figure 8C). Surprisingly, HG-DCA pigs with the worst clinical outcomes possessed a similar blood transcriptome profile to STG and STG-DCA pigs. HG pigs had increased levels of multiple genes related to energy metabolism and ATP synthesis, when compared with STG (Figure 8D) or HG-DCA pigs (Figure 8E), confirming that high circulating levels of glucose accelerated metabolic pathways to synthesize ATP, fueling infection responses. Conversely, reducing PN glucose intake from high to standard levels or DCA treatment during hyperglycemia conveyed transcriptional changes to the direction of less inflammation and energy metabolism. These findings, together with other data, imply that some detrimental impacts of DCA on the background of HG supply may stem from the more severe hyperglycemia induced by the inhibitory effects of DCA on blood cellular glucose uptake.

In summary, STG provision maintaining normoglycemia reduced the acute response to *S. epidermidis* infection and improved bacterial clearance relative to HG supply, but it did not provide the same protection against sepsis as bona fide glucose restriction. DCA treatment during infection efficiently dampened circulating aerobic glycolysis but did not further reduce sepsis severity. In contrast, on the background of HG supply, DCA treatment even exacerbated hyperglycemic and inflammatory conditions.

Discussion

The delicate balance of energy metabolism and immune response determines how neonates manage to survive serious infections (10). Here, we identified *S. epidermidis* dose thresholds for the host immunometabolic response in vitro and in vivo, and we uncovered the modulatory roles of systemic glucose provision and glycolysis in regulating inflammation and sepsis outcomes in a clinically relevant animal model of neonatal CONS bloodstream infection. First, the preterm cord blood response to bacteria was dose dependent, whereby

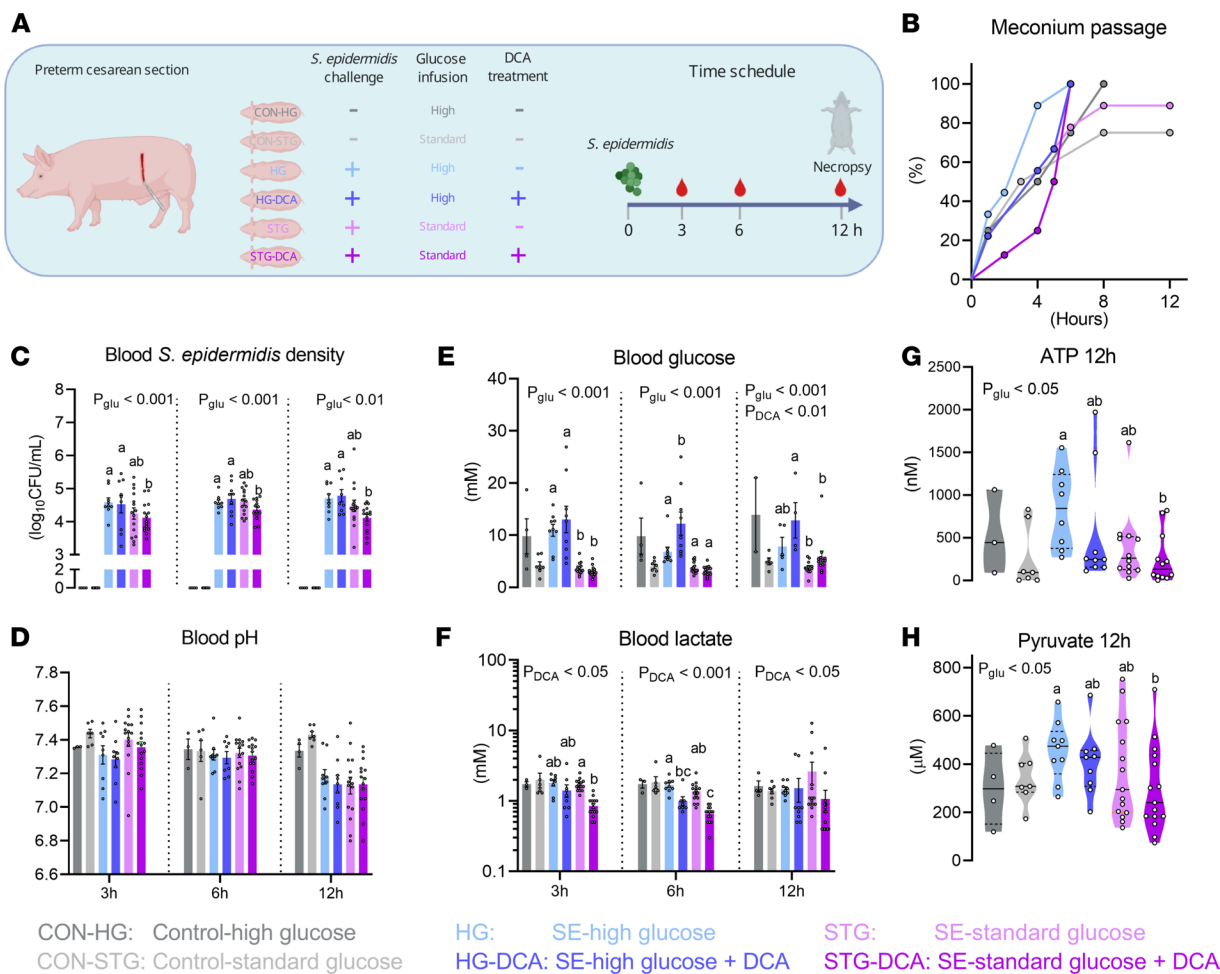


Figure 6. The impact of parenteral glucose levels and glycolysis inhibition by DCA on clinical response to *S. epidermidis* infection. (A) Preterm newborn piglets were nourished exclusively with PN containing HG (21%; 30 g/kg/d) or STG (10%; 14.4 g/kg/d) concentrations, intra-arterially infected with 10^9 CFU/kg *S. epidermidis*, followed by saline or DCA treatment (50 mg/kg) 30 minutes after infection ($n = 9-15$ /group). Uninfected animals receiving either HG or STG PN ($n = 4$ and 7 , respectively) served as references and were not included in the statistical analysis. (B) Time of first passed meconium after *S. epidermidis* infection. (C) *S. epidermidis* density from blood collected by jugular venous (at 3–6 hours) or heart (at 12 hours) puncture, by counting CFUs after plating onto tryptic soy agar containing 5% sheep's blood and incubated for 24 hours at 37°C. (D–F) Blood gas parameters in arterial blood at 3–12 hours. (G and H) Plasma ATP and pyruvate levels in heparinized plasma from arterial blood at 12 hours. (C–H) Data are presented as a cumulative hazard curve and analyzed by Mantel-Cox test (B), bar graphs including mean and SE (C–F) or violin dot plots including median and IQR (G and H), and analyzed separately at each blood sampling time point by linear mixed-effect model, including interaction between glucose and DCA. All analyzed data represent 3 independent litters. Among infected groups, the P_{DCA} and P_{glu} at each time point denote probability values for overall effects of DCA and glucose among the 4 infected groups in the linear mixed-effect model. Values at each blood-sampling time point not sharing the same letters are significantly different ($P < 0.05$). CON, control. Panel A was created using Biorender.com.

glycolysis and levels of inflammation markers increased and levels of OXPHOS markers decreased with increasing bacterial dose only until a certain dose, after which they were normalized to levels in controls. This demonstrates the Warburg effect in activated immune cells (34) with thresholds from immune tolerance to activation and, later, immunoparalysis. The response in preterm animals confirmed the trends of perturbed glucose homeostasis and activated glycolysis by infection with high bacterial doses leading to a high mortality rate. Second, a proof-of-concept study showed that high parenteral glucose provision during infection was clearly detrimental, via induced hyperglycemia, and accelerated glycolysis producing lactate and ATP, fueling inflammatory responses and leading to sepsis. In contrast, glucose restriction caused hypoglycemia but reduced inflammation and protected against sepsis. Third, in vitro glycolysis-inhibitor screening showed the efficacy of pyruvate dehydrogenase kinase inhibition by DCA to reduce inflammation and enhance OXPHOS and neutrophil phagocytosis. Finally, we found that the STG supply routinely used for preterm infants led to similar sepsis severity in infected animals, relative to HG supply, whereas DCA effects depended on levels of glucose supply. DCA increased inflammation and prompted more severe hyperglycemia during

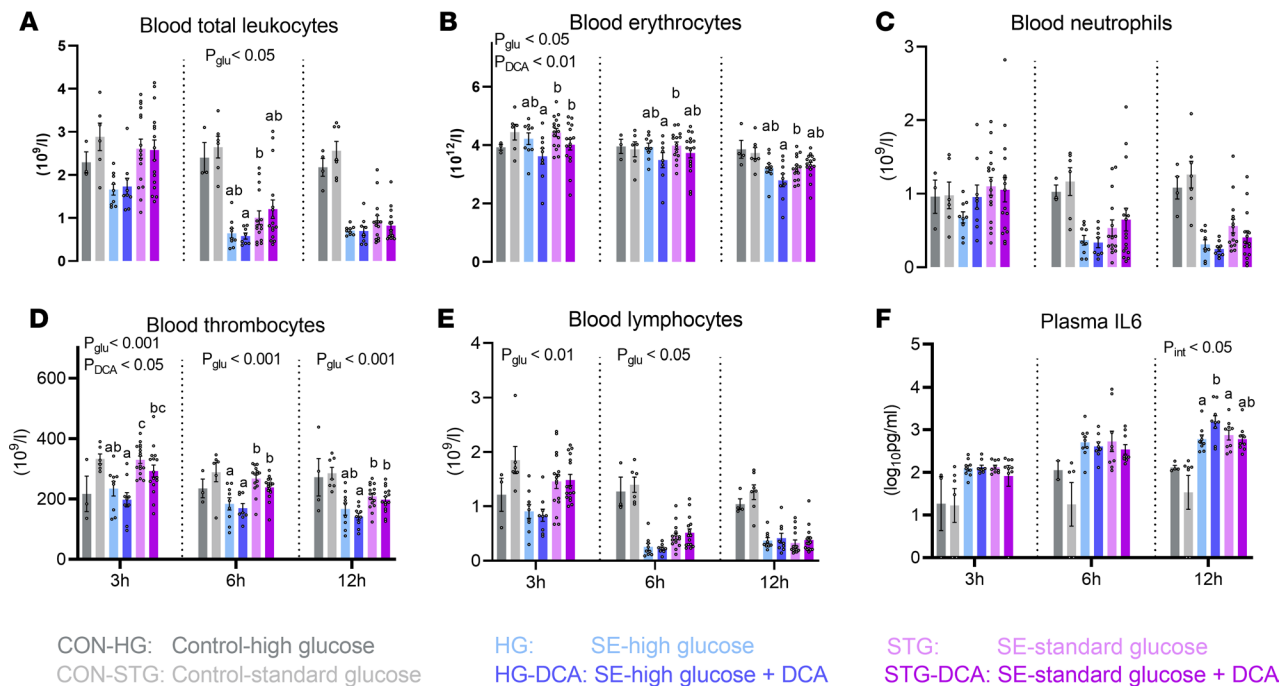


Figure 7. The impact of parenteral glucose levels and glycolysis inhibition by DCA on cellular and cytokine responses to *S. epidermidis* infection. (A-E) Numbers of hematopoietic cells and major leukocyte subsets in blood 3, 6, and 12 hours after *S. epidermidis* infusion. **(F)** Plasma IL-6 levels from the same blood samples. Data are presented as bar graphs with mean and SE and were analyzed separately for each blood sampling time using a linear mixed-effect model including glucose and DCA interaction. All analyzed data represent 3 independent experiments using separate litters. Among infected groups, P_{DCA} , P_{glu} , and P_{int} value for interaction [P_{int}] at each time point denote probability values for overall effects of DCA, glucose, and their interaction, respectively, among the 4 infected groups in the linear mixed-effect model. Values at each blood-sampling time point not sharing the same letters are significantly different ($P < 0.05$).

HG provision, whereas it decreased inflammation and improved bacterial clearance during STG provision, albeit without preventing sepsis. Our study suggests that parenteral glucose restriction could be a lifesaving therapy for infected preterm infants despite causing temporary hypoglycemia.

The tolerant status of preterm cord blood to low doses of *S. epidermidis* challenge in the study is in agreement with the impaired responses to LPS or bacteria of preterm versus term monocytes (12, 35) or that of preterm infants with sepsis compared with those without sepsis (4). On the other hand, increased bacterial dose beyond the resistant threshold decreased the ratio of pro- versus antiinflammatory genes, and normalized Treg levels and OXPHOS-related genes to those in controls, indicating the switch to immunoparalysis after blood cells used up all their energy stores. This response is similar to the immunosuppression in late stages of sepsis in infants and elderly persons (16, 36), predisposing them to secondary infections. To further test effects of glucose provision and pharmacological glycolysis inhibition, we selected the *S. epidermidis* dose exerting resistant responses and sepsis signs without significant acute mortality. Relative to infected animals with restricted parenteral glucose, those with high parenteral glucose supply had hyperglycemia, impaired bacterial clearance, hyper-inflammatory responses, and clinical signs of sepsis. Hyperglycemia in infected adult animals impairs monocyte chemotaxis and neutrophil phagocytosis, thereby decreasing bacterial clearance and increasing sepsis risk (37–39). The mechanism for this are unclear despite a few studies showing hyperglycemia-induced impaired IgG influx and complement protein release, which are needed for opsonization (40). Furthermore, hyperglycemia likely enhanced glucose uptake to accelerate glycolytic activity, in turn increasing lactate and ATP production used for inflammatory responses. Elevated glycolysis and impaired phagocytosis induced by hyperglycemia may explain high sepsis severity in these infected animals.

In contrast, restricted parenteral glucose caused hypoglycemia but prevented infected animals from elevated glycolysis, excessive inflammation, and sepsis. This solution may not be practical for hospitalized infants, because of the fear of hypoglycemia-induced brain injury (19). Importantly, we also showed the STG supply, which is routinely used in preterm infants (19), maintained normoglycemia but was not better than HG supply in protecting against sepsis, suggesting distinct beneficial glucose ranges for infected newborns (18). Therefore, we postulated that any other ways of reducing glycolysis may be

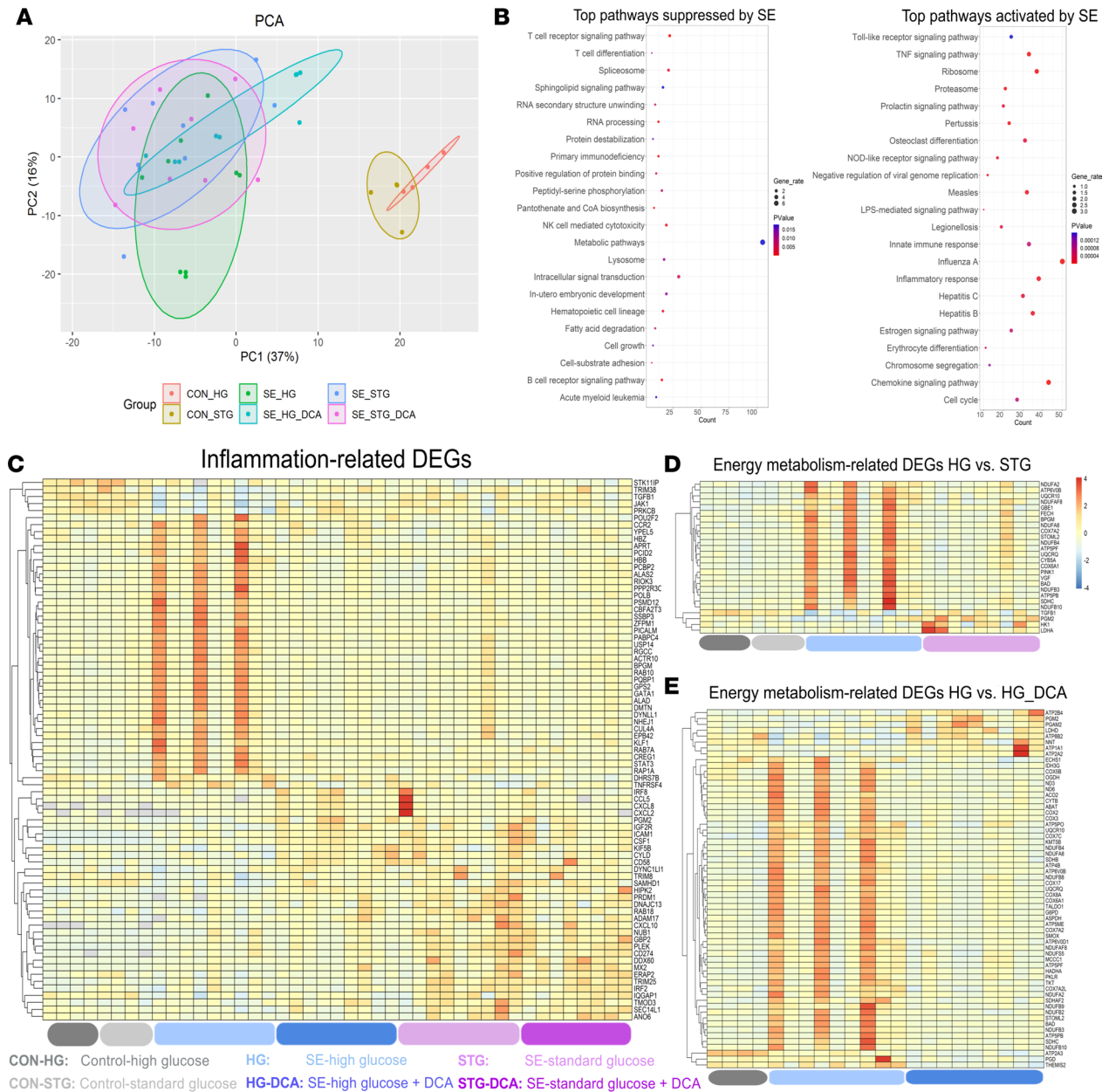


Figure 8. Blood transcriptomic responses to *S. epidermidis* infection and the effects of parenteral glucose levels and glycolysis inhibition by DCA. (A) Principal component (PC) analysis of the blood transcriptome at 12 hours in control (CON) or infected pigs nourished with a HG or STG parenteral regimen with or without DCA treatment. **(B)** The top pathways regulated by *S. epidermidis* (SE) infection analyzed by Kyoto Encyclopedia of Genes and Genomes and Gene Ontology pathway enrichment analysis using the Database for Annotation, Visualization, and Integrated Discovery database; DEG counts are displayed on the x-axis. **(C and D)** Heatmaps including inflammation- and energy metabolism-related DEGs between HG and STG animals. **(E)** Heatmap including energy metabolism-related DEGs between HG and HG-DCA animals. Analyses included 4 animals per control group and 8–9 per each infected group in 2 independent litters. For each DEG (row), z-scores of expression level were depicted in colors from blue (low) to red (high). All the statistics was performed by DESeq2 with FDR adjusted by BH procedure using $\alpha = 0.1$ as the threshold.

beneficial for both infection and sepsis outcomes without causing hypoglycemia. In principle, this was challenging, because phagocytes also depend on glycolysis to clear bacteria via phagocytosis (41–43). Via screening various drugs, we identified DCA with its short half-life that enhanced OXPHOS and decreased glycolysis, thereby potentially reducing ATP production and inflammation during infection (44, 45). DCA has also been used for adult patients with cancer (46). We found that DCA was detrimental in hyperglycemic infected animals but moderately beneficial in normoglycemic infected animals. Specifically, on a high PN glucose background, DCA induced more severe hyperglycemia, higher levels of inflammatory cytokines, and reduced bacterial clearance, suggesting its overall detrimental effects

likely derived from the decreased cellular glucose uptake during hyperglycemia. In contrast, DCA use on a standard parenteral glucose background dampened inflammation via its inhibitory effects on glycolysis and lactate production. Of note, despite evoking temporary glycolysis inhibition, DCA treatment during normoglycemia also enhanced *in vivo* bacterial clearance, likely via the enhanced neutrophil phagocytosis, as evidenced by transcriptomic analysis and phagocytosis test in DCA-treated cord blood and also in previous studies (47, 48). Clearly, the interaction between glucose supply and DCA mechanistic actions determined the inflammatory outcomes, suggesting the need for careful blood glucose monitoring during DCA use.

Importantly, standardized parenteral glucose supply, as recommended in the PN guideline for preterm infants (18, 19), with or without DCA treatment, could not prevent infected animals from showing clinical signs of sepsis, including acidemia (decreased blood pH) and respiratory acidosis (increased partial pressure of) despite ameliorated inflammatory effects. Our results thus suggest further refinement of the PN international guidelines, because the guidelines do not consider detailed PN glucose regimens during neonatal infection. Hence, there is a great need for clinical trials testing lower PN glucose provisions in infected preterm infants. If the lower-glucose recommended infusion rates cannot further decrease sepsis risk, as shown in this study, then additional restricted parenteral glucose infusion during neonatal infection may be warranted as a solution to prevent life-threatening sepsis despite causing temporary hypoglycemia.

Methods

S. epidermidis culture preparation and bacterial growth inhibitory assay. *S. epidermidis* (WT-1457, isolated from a patient with sepsis) was prepared from frozen stocks donated by Carina Mallard from the University of Gothenburg (Gothenburg, Sweden). Bacteria were previously cultured in heart infusion broth, and the stock bacterial concentration and OD were predetermined by CFU counting on blood agar plates following overnight incubation at 37°C. Right before *in vitro* experiments, the stock was thawed and diluted in PBS at 4°C to reach the desired levels. For *in vivo* experiments, 30 mL of tryptic soy broth was inoculated with 500 μ L of *S. epidermidis* stock and incubated for 17 hours at 37°C and 200 rpm. Culture OD was then measured by spectrophotometry and bacterial concentration estimated based on a previously established OD-to-CFU conversion factor. The culture was centrifuged for 20 minutes at 3000g and the bacterial pellet suspended in sterile physiological saline at 3×10^8 CFU/mL. The culture was plated onto tryptic soy agar and incubated overnight at 37°C to verify the actual concentration used in each experiment. For the bacterial growth inhibitory assay, *S. epidermidis* was cultured with the inoculated dose of 10^4 CFU/mL with and without immunometabolic drug addition, and bacterial density was determined at 0.5, 1, 2, 4, 6, 12, and 24 hours after inoculation.

In vitro cord blood stimulation with *S. epidermidis*. Cord blood collected at preterm pig delivery (day 106 of gestation, term at day 117 ± 2) was aliquoted into a sterile 96-well plate and stimulated with an increasing dose of *S. epidermidis* (5×10^1 to 5×10^7 cells/mL blood) at 37°C with 5% CO₂ for 2 hours. In some experiments, blood was preincubated with various concentrations of glycolysis inhibitors (namely, rapamycin, DCA, and FX11, all from Sigma-Aldrich). After stimulation, a blood fraction was stabilized with a mixture of lysis/binding solution and isopropanol (MagMAX 96 Blood RNA Isolation Kit; ThermoFisher), and stored at -80°C for RNA analyses. The remaining blood was centrifuged (2000g, 10 minutes, 4°C), and plasma analyzed for cytokines and metabolic targets. In some experiments, cord blood after stimulation was used for flow cytometry analysis of CD4⁺Foxp3⁺ lymphocytes (Tregs) or plated onto agar plate for estimation of bacterial density. All *in vitro* experiments were performed using cord blood from at least 4 preterm animals.

In vivo *S. epidermidis* infection in preterm pigs. All piglets (crossbred, Landrace \times Yorkshire \times Duroc) were delivered by elective cesarean section at gestational day 106 (~90% gestation). The sow's anesthesia and surgical procedures are described in detail elsewhere (49). After delivery, the animals were housed singly in ventilated, heated (37°C) incubators with oxygen supply (1 L/min). For resuscitation, animals received doxapram and flumazenil (0.1 mL/kg each drug, *i.m.*) and positive airway pressure ventilation until breathing stabilized. Thereafter, a 4F catheter was inserted into 1 of the umbilical arteries under aseptic conditions and fixed at the level of the descending aorta for provision of PN, *S. epidermidis* inoculation, and blood sampling. Successfully resuscitated animals were stratified by sex and birth weight and were randomly allocated into treatment groups. In all animal experiments, *S. epidermidis* was administered intra-arterially as a 3-minute continuous infusion (3.33 mL/kg), using a precision infusion pump, within 4 hours after birth. Throughout the whole experiment, from birth to euthanasia,

the animals were nourished parenterally with Kabiven infusion formula (fats: 3.1%, 4.5 g/kg/d; amino acids: 4.5%, 6.5 g/kg/d; and varying glucose concentrations: 1.4%–21%, 2–30 g/kg/d; Fresenius-Kabi) at infusion rates of 6 mL/kg/h. The nutritional composition of PN and fluid support across groups was identical except the glucose content (Supplemental Table 3). Animals were permanently monitored by experienced caretakers for the duration of the experiments (12–24 hours) and euthanized preschedule (at the humane endpoint) if an animal had clinical and paraclinical signs of sepsis (defined as arterial blood pH < 7.1 and clinical symptoms of extreme lethargy, discoloration, and hypoperfusion). Blood was collected by jugular venous or heart puncture on sterilized skin for bacteriology and through the umbilical catheter for the remaining analytical endpoints. Scheduled euthanasia was preceded by deep anesthesia, followed by a lethal dose of intracardiac barbiturate. Animal caretakers were not blinded to the respective treatment groups, but all endpoint and data analyses (except meconium passage time) were conducted in a blinded fashion.

In the initial, in vivo, bacterial dose-response experiment that served to establish a clinical and metabolic phenotype, animals were randomly allocated to receive saline (control, $n = 13$), 10^6 ($n = 7$), 10^8 ($n = 14$), 10^9 ($n = 10$), or 5×10^9 ($n = 13$) CFU/kg *S. epidermidis*. Animals were nourished with PN containing an STG concentration (10%), corresponding to a daily glucose intake of 14.4 g/kg, and monitored for 24 hours, including during blood collection at 12 and 24 hours. To confirm the in vivo metabolic responses to infection, a follow-up experiment was conducted in control ($n = 6$) and infected animals ($n = 12$; 10^9 CFU/kg), and collected liver after euthanasia 12 hours after infection was used for transcriptomic analysis.

In the subsequent experiment addressing the hypothesis that glucose restriction protected against sepsis, animals were randomly allocated to receive 10^9 CFU/kg *S. epidermidis* and PN formula containing either a LG (1.4% or 2 g/kg/d; $n = 10$) or HG (21% or 30 g/kg/d; $n = 11$) concentration. A third piglet group of reduced sample size served as uninfected controls ($n = 3$) and received LG (1.4%) parenteral formulation. All animals were monitored for 12 hours, including during blood collection at 3, 6, and 12 hours.

The final experiment addressed the hypothesis that reducing PN glucose intake from high to standard regimens with or without indirect glycolysis inhibition via DCA administration (directly inhibiting pyruvate dehydrogenase kinase 1) would protect against sepsis. Animals were randomly allocated to receive 10^9 CFU/kg *S. epidermidis* and PN containing STG concentration (10%, 14.4 g/kg/d; $n = 15$) without DCA or STG-DCA ($n = 15$), or PN with HG concentration without DCA (21%; $n = 9$) or HG-DCA ($n = 9$). DCA groups received 50 mg/kg (i.e., 1 mL solution per kg) DCA intra-arterially exactly 30 minutes after *S. epidermidis* infusion, whereas DCA controls received an equivalent volume of sterile saline. Some infected STG-DCA animals ($n = 7$) also received additional DCA (50 mg/kg) at 3 and 6 hours after infection, but they showed no additional effects relative to those with single DCA treatment; therefore, they were pooled to form the STG-DCA group. Besides, animals were randomly allocated to 2 uninfected control groups receiving either standard (control-STG; $n = 7$) or high PN glucose (control-HG; $n = 4$). The animals were monitored for 12 hours, including during blood sampling at 3, 6, and 12 hours.

CD4⁺Foxp3⁺ lymphocytes and neutrophil phagocytosis. In an in vitro experiment, the frequency of CD4⁺Foxp3⁺ lymphocytes (a marker for Tregs) in *S. epidermidis*-stimulated blood was analyzed (30). Briefly, stimulated blood was lysed to remove erythrocytes, washed with PBS, permeabilized, blocked with porcine serum (ThermoFisher), and stained with a mixture of FITC-conjugated mouse-IgG2 β anti-porcine CD4 Ab (clone MIL17), APC-conjugated rat-IgG2 α anti-porcine Foxp3 Ab (clone FJK-16s), and analyzed by a BD Accuri C6 flow cytometer (BD Biosciences). In another experiment, cord blood preincubated with the glycolysis inhibitor DCA under different glycemic conditions was assessed for its phagocytosis capacity, as previously described (50). In brief, glucose-supplemented cord blood was stimulated with pHrodo red-conjugated *E. coli* bioparticles (Phagocytosis Kit; ThermoFisher) at 37°C for 30 minutes, followed by flow cytometry analysis, as mentioned above. The percentage of neutrophils having phagocytic capacity in the total number of neutrophils was evaluated.

Gene expression analysis by qPCR and whole-transcriptome shotgun sequencing. Total whole-blood and liver RNA from in vitro and in vivo experiments was extracted using the MagMAX 96 Blood RNA Isolation Kit. RNA was then converted to cDNA with the High-Capacity cDNA Reverse Transcription Kit (Applied Biosystems). Transcription of selected genes related to inflammation, innate and adaptive immunity, and energy metabolisms were determined by qPCR using QuantiTect SYBR Green PCR Kit (Qiagen) on the LightCycler 480 System (Roche) with predesigned primers (sequences are listed in Supplemental Table 2I). Primers were designed with the Gene database and Primer-BLAST software (National Center for Biotechnology Information). Relative expression of target genes was calculated by $\Delta\Delta$ Ct method with HPRT1 serving as the housekeeping gene.

Whole-blood RNA from selected samples from *in vitro* and *in vivo* experiments was analyzed by whole-transcriptome shotgun sequencing (30) to profile immunometabolic pathways affected by relevant interventions. Briefly, RNA-Seq libraries were constructed using 1000 ng of RNA and the VAHTS mRNA-Seq V3 Library Prep Kit for Illumina (Vazyme). The libraries were sequenced on the Illumina NovaSeq 6000 platform to generate 150 bp paired-end reads. Quality and adapter trimming of raw reads were performed using TrimGalore (Babraham Bioinformatics). The remaining clean reads (~26 million/sample) were aligned to the porcine genome (Sscrofa11.1) using Tophat2 (51). The annotated gene information of porcine genome was obtained from Ensembl (release 99). The script htseq-count (52) was used to generate a gene-count matrix, followed by analyses of DEGs using DESeq2 (53). Sequencing data are deposited in the Gene Expression Omnibus with accession number GSE201554.

Plasma cytokines and metabolic targets. Plasma from *in vitro* and *in vivo* experiments was analyzed for porcine-specific cytokines using ELISA (TNF- α [DY690B], IL-10 [DY693B], and IL-6 [DY686], porcine DuoSet; R&D Systems) and targets related to energy metabolism. Glucose and lactate levels were measured by Glucose Assay Kit and Lactate Assay Kit, respectively (all from Nordic BioSite). Extracellular ATP and pyruvate levels were measured by the ATP Colorimetric/Fluorometric Assay Kit and the Pyruvate Assay Kit (Sigma-Aldrich).

Statistics. All continuous data were analyzed using R Studio, version 3.4.1 software. *In vitro* data were analyzed by a linear mixed-effect model with treatment as a fixed factor and pig identification number (ID) as a random factor, followed by Tukey post hoc pair-wise comparisons. Survival curves (meconium passages or survival) were analyzed using Mantel-Cox log-rank tests. To compare HG and LG infected animals, each parameter was fitted into a linear mixed-effect model with glucose level, time, and their interaction as fixed factors and litter and pig ID as random factors, using the *lme4* and *multcomp* packages (54). Group comparisons at each time point were also performed with similar models without the contributing factors of time of blood sampling and pig ID. For the experiment identifying glucose and DCA effects in infected animals, each parameter at each blood sampling time point was fitted into a linear mixed-effect model with glucose, DCA, and their interaction as fixed factors and pig ID as a random factor. For pair-wise comparisons, the Tukey post hoc test was used after a linear mixed-effect model was applied with treatment as a fixed factor and litter as random factor. An adjusted *P* value of <0.05 was regarded as statistically significant. Data are presented as violin dot plots with median and IQR. All reported measures were evaluated for normal distribution, and logarithmic transformation was performed if necessary.

For transcriptomics, significant DEGs among groups were identified by DESeq2 using a Benjamini-Hochberg (BH) adjusted *P* value of <0.1 as the cutoff. To control type I error, *P* value tests were further adjusted by FDR ($\alpha = 0.1$) into *q* values (55). For blood transcriptomics, gene ontology and Kyoto Encyclopedia of Genes and Genomes pathway enrichment analyses for DEGs were performed using the Database for Annotation, Visualization, and Integrated Discovery (56), and a BH-adjusted *P* value of <0.05 was considered statistically significant. For liver transcriptomics, gene set enrichment analysis (GSEA) for DEGs was performed using the *fgsea* package with R Studio, version 3.4.1 and GSEA, version 4.2.2 (UCSD and Broad Institute) (57), and pathways with an adjusted *P* value of <0.05 were considered statistically significant. Lists of genes with mean expression levels and adjusted *P* values, as well as enriched pathways with associated DEGs, are listed for each comparison from *in vivo* (Supplemental Table 1, A–K), and *in vitro* (Supplemental Table 2, A–H) experiments. Heatmaps were generated using R package *pheatmap*.

Study approval. The animal studies and experimental procedures were approved by the Danish Animal Experiments Inspectorate (license no. 2020-15-0201-00520), which complies with the European Union Directive 2010/63 (legislation for the use of animals in research).

Author contributions

DNN designed the study. TK, AB, NLH, KAS, and DNN performed the animal experiments and laboratory analyses. TM, AB, and DNN conducted bioinformatics, statistical analyses, and data interpretation. TM and AB managed raw data and generated all figures and tables. TM, AB, and DNN drafted the manuscript. All authors contributed to data interpretation, manuscript revision, and approval of the final manuscript version. The levels of contribution in study design, actual experiments, laboratory analyses, and writing were used to assign co-first authorship order.

Acknowledgments

The study was supported by the University of Copenhagen. The authors thank Per Sangild, Thomas Thymann, Ole Bæk, Rene L. Shen, Xiaoyu Pan, Britta Karlsson, and Jane C. Povlsen for the assistance in animal experiments and omics data acquisition.

Address correspondence to: Duc Ninh Nguyen, Section for Comparative Pediatrics and Nutrition, Department of Veterinary and Animal Sciences, University of Copenhagen, Dyrlægevej 68, DK-1870 Frederiksberg C, Denmark. Phone: 45.35333250; Email: dnn@sund.ku.dk.

1. Strunk T, et al. Infection-induced inflammation and cerebral injury in preterm infants. *Lancet Infect Dis*. 2014;14(8):751–762.
2. Dong Y, Speer CP. Late-onset neonatal sepsis: recent developments. *Arch Dis Child Fetal Neonatal Ed*. 2015;100(3):F257–F263.
3. Dong Y, et al. Beyond sepsis: Staphylococcus epidermidis is an underestimated but significant contributor to neonatal morbidity. *Virulence*. 2018;9(1):621–633.
4. Strunk T, et al. Impaired cytokine responses to live Staphylococcus epidermidis in preterm infants precede gram-positive, late-onset sepsis. *Clin Infect Dis*. 2020;72(2):271–278.
5. Mittendorf R, et al. Association between cerebral palsy and coagulase-negative staphylococci. *Lancet*. 1999;354(9193):1875–1876.
6. Gray JE, et al. Coagulase-negative staphylococcal bacteremia among very low birth weight infants: relation to admission illness severity, resource use, and outcome. *Pediatrics*. 1995;95(2):225–230.
7. Clark RH, et al. Empiric use of ampicillin and cefotaxime, compared with ampicillin and gentamicin, for neonates at risk for sepsis is associated with an increased risk of neonatal death. *Pediatrics*. 2006;117(1):67–74.
8. Stoll BJ, et al. Very low birth weight preterm infants with early onset neonatal sepsis: the predominance of gram-negative infections continues in the National Institute of Child Health and Human Development Neonatal Research Network, 2002–2003. *Pediatr Infect Dis J*. 2005;24(7):635–639.
9. Becattini S, et al. Antibiotic-induced changes in the intestinal microbiota and disease. *Trends Mol Med*. 2016;22(6):458–478.
10. Harbeson D, et al. Energy demands of early life drive a disease tolerant phenotype and dictate outcome in neonatal bacterial sepsis. *Front Immunol*. 2018;9:1918.
11. Conti MG, et al. Immunometabolic approaches to prevent, detect, and treat neonatal sepsis. *Pediatr Res*. 2020;87(2):399–405.
12. Kan B, et al. Cellular metabolism constrains innate immune responses in early human ontogeny. *Nat Commun*. 2018;9(1):4822.
13. Dreschers S, et al. Impaired cellular energy metabolism in cord blood macrophages contributes to abortive response toward inflammatory threats. *Nat Commun*. 2019;10(1):1685.
14. Levy O, et al. Selective impairment of TLR-mediated innate immunity in human newborns: neonatal blood plasma reduces monocyte TNF-alpha induction by bacterial lipopeptides, lipopolysaccharide, and imiquimod, but preserves the response to R-848. *J Immunol*. 2004;173(7):4627–4634.
15. Sadeghi K, et al. Immaturity of infection control in preterm and term newborns is associated with impaired toll-like receptor signaling. *J Infect Dis*. 2007;195(2):296–302.
16. Hibbert JE, et al. Sepsis-induced immunosuppression in neonates. *Front Pediatr*. 2018;6:357.
17. McGuire W, et al. Feeding the preterm infant. *BMJ*. 2004;329(7476):1227–1230.
18. Alaedeen DI, et al. Total parenteral nutrition-associated hyperglycemia correlates with prolonged mechanical ventilation and hospital stay in septic infants. *J Pediatr Surg*. 2006;41(1):239–244.
19. Mesotten D, et al. ESPGHAN/ESPEN/ESPR/CSPEN guidelines on pediatric parenteral nutrition: carbohydrates. *Clin Nutr*. 2018;37(6 pt b):2337–2343.
20. Harris DL, et al. Incidence of neonatal hypoglycemia in babies identified as at risk. *J Pediatr*. 2012;161(5):787–791.
21. Rozance PJ, Hay WW. Neonatal hyperglycemia. *Neoreviews*. 2010;11(11):e632–e639.
22. Beardsall K, et al. Prevalence and determinants of hyperglycemia in very low birth weight infants: cohort analyses of the NIRTURE study. *J Pediatr*. 2010;157(5):715–719.
23. Hubbard WJ, et al. Cecal ligation and puncture. *Shock*. 2005;24 Suppl 1:52–57.
24. Singer JR, et al. Preventing dysbiosis of the neonatal mouse intestinal microbiome protects against late-onset sepsis. *Nat Med*. 2019;25(11):1772–1782.
25. Knoop KA, et al. Maternal activation of the EGFR prevents translocation of gut-residing pathogenic *Escherichia coli* in a model of late-onset neonatal sepsis. *Proc Natl Acad Sci U S A*. 2020;117(14):7941–7949.
26. Brunse A, et al. Oral supplementation with bovine colostrum prevents septic shock and brain barrier disruption during bloodstream infection in preterm newborn pigs. *Shock*. 2018;51(3):337–347.
27. Burrin D, et al. Translational advances in pediatric nutrition and gastroenterology: new insights from pig models. *Annu Rev Anim Biosci*. 2020;8:321–354.
28. Sangild PT, et al. Diet- and colonization-dependent intestinal dysfunction predisposes to necrotizing enterocolitis in preterm pigs. *Gastroenterology*. 2006;130(6):1776–1792.
29. Nguyen DN, et al. Prenatal intra-amniotic endotoxin induces fetal gut and lung immune responses and postnatal systemic inflammation in preterm pigs. *Am J Pathol*. 2018;188(11):2629–2643.
30. Ren S, et al. Prenatal inflammation suppresses blood Th1 polarization and gene clusters related to cellular energy metabolism in preterm newborns. *FASEB J*. 2020;34(2):2896–2911.
31. James MO, et al. Therapeutic applications of dichloroacetate and the role of glutathione transferase zeta-1. *Pharmacol Ther*. 2017;170:166–180.
32. Ohashi T, et al. Dichloroacetate improves immune dysfunction caused by tumor-secreted lactic acid and increases antitumor immunoreactivity. *Int J Cancer*. 2013;133(5):1107–1118.

33. Stacpoole PW, et al. Treatment of lactic acidosis with dichloroacetate. *N Engl J Med.* 1983;309(7):390–396.
34. O'Neill LAJ, et al. A guide to immunometabolism for immunologists. *Nat Rev Immunol.* 2016;16(9):553–565.
35. De Jong E, et al. Identification of generic and pathogen-specific cord blood monocyte transcriptomes reveals a largely conserved response in preterm and term newborn infants. *J Mol Med (Berl).* 2018;96(2):147–157.
36. Boomer JS, et al. Immunosuppression in patients who die of sepsis and multiple organ failure. *JAMA.* 2011;306(23):2594–2605.
37. Javid A, et al. Hyperglycemia impairs neutrophil-mediated bacterial clearance in mice infected with the Lyme disease pathogen. *PLoS One.* 2016;11(6):e0158019.
38. Gan Y-H. Host susceptibility factors to bacterial infections in type 2 diabetes. *PLoS Pathog.* 2013;9(12):e1003794.
39. Watanabe Y, et al. Exogenous glucose administration impairs glucose tolerance and pancreatic insulin secretion during acute sepsis in non-diabetic mice. *PLoS One.* 2013;8(6):e67716.
40. Mauriello CT, et al. Hyperglycemia inhibits complement-mediated immunological control of *S. aureus* in a rat model of peritonitis. *J Diabetes Res.* 2014;2014:762051.
41. Kumar S, Dikshit M. Metabolic insight of neutrophils in health and disease. *Front Immunol.* 2019;10:2099.
42. Pence BD, Yarbrow JR. Classical monocytes maintain ex vivo glycolytic metabolism and early but not later inflammatory responses in older adults. *Immun Ageing.* 2019;16(1):3.
43. Diskin C, Pålsson-McDermott EM. Metabolic modulation in macrophage effector function. *Front Immunol.* 2018;9:270.
44. Eleftheriadis T, et al. Dichloroacetate at therapeutic concentration alters glucose metabolism and induces regulatory T-cell differentiation in alloreactive human lymphocytes. *J Basic Clin Physiol Pharmacol.* 2013;24(4):271–276.
45. McCall CE, et al. Pyruvate dehydrogenase complex stimulation promotes immunometabolic homeostasis and sepsis survival. *JCI Insight.* 2018;3(15):99292.
46. Fujiwara S, et al. PDK1 inhibition is a novel therapeutic target in multiple myeloma. *Br J Cancer.* 2013;108(1):170–178.
47. Dikalov S. Crosstalk between mitochondria and NADPH oxidases. *Free Radic Biol Med.* 2011;51(7):1289–1301.
48. Hassoun EA, Dey S. Dichloroacetate- and trichloroacetate-induced phagocytic activation and production of oxidative stress in the hepatic tissues of mice after acute exposure. *J Biochem Mol Toxicol.* 2008;22(1):27–34.
49. Brunse A, et al. Enteral broad-spectrum antibiotics antagonize the effect of fecal microbiota transplantation in preterm pigs. *Gut Microbes.* 2021;13(1):1–16.
50. Ren S, et al. Gut and immune effects of bioactive milk factors in preterm pigs exposed to prenatal inflammation. *Am J Physiol Gastrointest Liver Physiol.* 2019;317(1):G67–G77.
51. Kim D, et al. TopHat2: accurate alignment of transcriptomes in the presence of insertions, deletions and gene fusions. *Genome Biol.* 2013;14(4):R36.
52. Anders S, et al. HTSeq—a Python framework to work with high-throughput sequencing data. *Bioinformatics.* 2015;31(2):166–169.
53. Love MI, et al. Moderated estimation of fold change and dispersion for RNA-seq data with DESeq2. *Genome Biol.* 2014;15(12):550.
54. Bates D, et al. Fitting linear mixed-effects models using lme4. <https://arxiv.org/abs/1406.5823>. Accessed May 3, 2022.
55. Pollard KS, et al. Resampling-based multiple hypothesis testing. <https://bioconductor.org/packages/multtest/>. Accessed May 3, 2022.
56. Huang DW, et al. Bioinformatics enrichment tools: paths toward the comprehensive functional analysis of large gene lists. *Nucleic Acids Res.* 2009;37(1):1–13.
57. Subramanian A, et al. Gene set enrichment analysis: a knowledge-based approach for interpreting genome-wide expression profiles. *Proc Natl Acad Sci U S A.* 2005;102(43):15545–15550.